LEGIBILITY NOTICE

A major purpose of the Technical Information Center is to provide the broadest dissemination possible of information contained in DOE's Research and Development Reports to business, industry, the academic community, and federal, state and local governments.

Although a small portion of this report is not reproducible, it is being made available to expedite the availability of information on the research discussed herein.

CONF

CONF-810874--2

LA-UR-81-2737

LA-UR--81-2737

DE82 000564

TITLE: INITIATION OF PROPAGATING DETONATIONS

MASTER

AUTHOR(S): Charles L. Mader

SUBMITTED TO: Eighth International Colloquium on Gasdynamics of Explosions and Reactive Systems

University of California

LOS ALAMOS SCIENTIFIC LABORATORY
Post Office Box 1663 Los Alamos, New Mexico 87545
An Affirmative Action/Equal Opportunity Employer

Form No. 836 R3
St. No. 2629
12/78

UNITED STATES
DEPARTMENT OF ENERGY
CONTRACT W-7405-ENG. 36

Initiation of propagating detonations

Charles L. Mader

Los Alamos National Laboratory

Los Alamos, New Mexico 87544

Abstract--The initiation of propagating detonation in PBX 9404, PBX 9502, and X0219 by hemispheric initiators of PBX 9404, 1.8 g/cm^3-TATB, and X0351 is described numerically, using the two-dimensional Lagrangian code, 2DL, and the Forest Fire rate to describe the heterogeneous explosive shock initiation process. The initiation of propagating detonation in the insensitive explosive PBX 9502 by triple-shock-wave interaction from three initiators has been modeled using the three-dimensional, reactive, Eulerian hydrodynamic code, 3DE.

1. Introduction

The initiation of propagating, diverging detonation is usually accomplished by small conventional initiators; however, as the explosive to be initiated becomes more shock insensitive, the initiators must have larger diameters (>2.5 cm) to be effective.

The I^{2}C camera was used to examine the nature of the diverging detonation waves formed in PBX 9404 (94/3/3 HMX/nitrocellulose/Tris-β-chloroethyl phosphate), X0290 or PBX 9502 (95/5 TATB/Kel-F at 1.894 g/cm^3) and X0219 (90/10 TATB/Kel-F at 1.914 g/cm^3) by hemispheric initiators.† The geometries of the initiators were (1) a 6.35-mm-radius hemisphere of PBX 9407

†These data were supplied by James R. Travis, Los Alamos National Laboratory Group M-3.

(94/6 RDX/Exon at 1.61 g/cm^3) surrounded by a 6.35-mm-thick hemisphere of PBX 9404, (2) a 6.35-mm-radius hemisphere of 1.7-g/cm^3 TATB surrounded by a 19.05-mm-thick hemisphere of 1.8-g/cm^3 TATB, or (3) a 16-mm-radius hemisphere of X0351 (15/5/80 HMX/Kel-F/TATB at 1.89 g/cm^3).

We have numerically examined systems with similar geometries by use of the hydrodynamic code 2DL [1] and the Forest Fire rate [1] to describe the shock initiation process. As the explosive to be initiated becomes more shock insensitive, the initiators must have larger diameters or some other method must be used to achieve the required high pressures of adequate duration. High pressures are achieved if two or more shock waves interact to form regular or Mach shock reflections. We will investigate propagating detonation initiation in the insensitive high explosive PBX 9502 by the double- and triple-wave interaction of shock waves formed by initiators that are too weak to initiate propagating detonation individually.

2. Numerical modeling of initiation by single initiators

The two-dimensional, reactive, Lagrangian hydrodynamic code 2DL was used to describe the reactive fluid dynamics. The Forest Fire description of heterogeneous shock initiation was used to describe explosive burn. The HOM equation of state and Forest Fire rate constants for PBX 9502, PBX 9404, and X0219 were identical to those described in Ref. [1]. The Pop plots are shown in Fig. 1 and the Forest Fire rates in Fig. 2. The BKW detonation product equation-of-state constants for X0351 and for 1.7- and 1.8-g/cm^3 TATB are given in Ref. [2].

The calculations were done in cylindrical geometry with Lucite confinement rather than the air confinement present in the experimental study. The Lucite confinement prevents the mesh distortion that can be fatal to Lagrangian calculations.

The central 6.35-mm region of the detonator is initially exploded, which initiates the remaining explosive in the detonator using a C-J volume burn. For any given mesh size and time step, the viscosity must be adjusted to give a peak pressure at the detonation front near the effective C-J pressure. The parameters used are as follows.

Calculation		Mesh Size	Time Step	Viscosity
Initiator	Acceptor	(cm)	(μs)	Coefficient
PBX 9407/PBX 9404	PBX 9404	0.05	0.02	4.0
PBX 9407/PBX 9404	PBX 9502	0.05	0.02	3.5
PBX 9407/PBX 9404	X0219	0.05	0.02	4.2
1.7 TATB/1.8 TATB	PBX 9502	0.1	0.02	5.0
X0351	PBX 9502	0.1	0.02	5.0

The pressure and mass fraction contours are shown for a PBX 9404 hemisphere initiating PBX 9404 in Fig. 3, PBX 9502 (X0290) in Fig. 4, and X0219 in Fig. 5. The experimental and calculated position of the leading wave as a function of distance from the origin is shown in Fig. 6.

The burn can become unstable when it turns a corner. The instability is apparently numerical because it can be eliminated by using an average of nearby cell pressures for the Forest Fire burn rather than the individual cell pressure.

The pressure and mass fraction contours are shown in Fig. 7 for the 1.8-g/cm^3 TATB hemisphere initiating PBX 9502. Very little undecomposed explosive was observed experimentally, in agreement with the calculated results. The contours are shown in Fig. 8 for an X0351 hemisphere initiating PBX 9502. The experimental and calculated regions of partially decomposed PBX 9502 are shown in Fig. 9.

3. Numerical modeling of initiation by multiple initiators

The three-dimensional Eulerian hydrodynamic computer code, 3DE, [3] was used to model numerically the interaction of shock waves in PBX 9502 formed by initiators that are too small to initiate propagating detonation. The calculations were performed on the CRAY computer. The Forest Fire model of heterogeneous explosive shock initiation was used to describe the explosive burn.

The geometry studied is shown in Fig. 10. Two or three initiator cubes of 7 by 7 by 7 cells are placed symmetrically in a PBX 9502 cube with continuum boundaries on its sides. The initiator cube centers were 1.6 cm apart and 1.09 cm from the cube bottoms. The indices i, j, and k designate the position of the x-, y-, and z-coordinates. The total cube height is k of 31, i is 29, and j is 25. The initiator cubes were initially decomposed PBX 9502 with a 2.5-g/cm^3 initial density, which has an initial pressure of 245 kbar. This sends a diverging ~100-kbar shock into the surrounding PBX 9502. The computational cell size used was 0.114 cm, and the time step was 0.022 μs. The computer time for the 22,475 cells was about 50 minutes for 150 cycles.

The expected wave interactions are sketched in Fig. 11. The sketch shows the waves, just after double-wave interaction, as dashed lines, and the dark region shows the double-wave interactions. The solid lines and dotted regions show the waves after triple-wave interaction.

The pressures from the diverging double-wave interaction in inert PBX 9502 are about 200 kbar, and those from the triple-wave interaction are about 300 kbar.

The calculated three-dimensional pressure and mass fraction contours for two initiators are shown in Fig. 12 and for three initiators in Fig. 13.

The isobar and mass fraction cross sections for layer j of 9 (across the detonator centers) are shown for two initiators in Fig. 14 at 1.34 μs, in Fig. 15 at 1.78 μs, and in Fig. 16 at 2.66 μs. The isobar and mass fraction cross sections for layer j of 11 (across the edge of the detonators) for three initiators are shown in Fig. 17 at 1.78 μs, in Fig. 18 at 3.10 μs, and in Fig. 19 at 4.42 μs.

Although two initiators cause double-wave interaction that results in considerable decomposition, propagating detonation does not result.

Three initiators fail to initiate propagating detonation at the double-wave interaction points but do at the triple-wave interaction region. The higher triple-wave interaction pressure results in a shorter run to detonation. The detonation can be maintained long enough to become a propagating, diverging detonation.

4. Conclusions

The initiation of propagating detonation in sensitive (PBX 9404) and insensitive (PBX 9502 and X0219) explosives by hemispheric initiators can be described numerically using the two-dimensional Lagrangian code 2DL and the Forest Fire rate. Large regions of partially decomposed explosive occur even when insensitive explosives are initiated by large initiators.

The three-dimensional Eulerian hydrodynamic computer code, 3DE, has been used to examine the interaction of two and three shock waves from initiators in PBX 9502. The dynamics of initiating propagating detonation in an insensitive explosive by multiple shock-wave interactions has been modeled numerically.

References

1. Mader, Charles L. (1979) Numerical Modeling of Detonations, University of California Press, Berkeley.

2. Mader, Charles L., Numerical Modeling of Insensitive High-Explosive Initiators, Los Alamos Scientific Laboratory report LA-8437-MS (1980).

3. Mader, Charles L. and Kershner, J. D., Three-Dimensional Eulerian Calculations of Triple-Initiated PBX 9404, Los Alamos Scientific Laboratory report LA-8206 (1980).

Figure captions

1. The distance of run to detonation as a function of the shock pressure.
2. The Forest Fire decomposition rates as a function of shock pressure.
3. The pressure and mass fraction contours at various times for a hemispheric initiator of 6.35-mm-radius PBX 9407 surrounded by 6.35 mm of PBX 9404 initiating PBX 9404. The pressure contour interval is 50 kbar and the mass fraction contour is 0.1.
4. The pressure and mass fraction contours at various times for a hemispheric initiator of 6.35-mm-radius PBX 9407 surrounded by 6.35 mm of PBX 9404 initiating PBX 9502 (X0290). The pressure contour interval is 50 kbar and the mass fraction contour is 0.1.
5. The pressure and mass fraction contours at various times for a hemispheric initiator of 6.35-mm-radius PBX 9407 surrounded by 6.35 mm of PBX 9404 initiating X0219. The pressure contour interval is 50 kbar and the mass fraction contour is 0.1.
6. The experimental and calculated position of the leading wave from the top of the explosive block as a function of the distance of the leading front of the wave from the origin.
7. The pressure and mass fraction contours at various times for a hemispheric initiator of 6.35-mm-radius TATB at 1.7 g/cm^3 surrounded by 19.05 mm of TATB at 1.8 g/cm^3 initiating PBX 9502. The pressure contour interval is 50 kbar and the mass fraction contour is 0.1.
8. The pressure and mass fraction contours at various times for a hemispheric initiator of 16-mm-radius X0351 initiating PBX 9502. The pressure contour interval is 50 kbar and the mass fraction contour is 0.1.
9. The calculated and experimental region of partially decomposed PBX 9502 when initiated by an X0351 initiator.

Figure captions (cont)

10. A PBX 9502 cube with three embedded rectangular initiators.
11. The expected double- and triple-wave interactions from three initiators. The dashed lines and dark regions show the double-wave interaction. The solid lines and dotted regions show the triple-wave interaction.
12. The calculated three-dimensional pressure and mass fraction contours for two initiators in PBX 9502. The pressure contours are shown for 200, 150, and 100 kbar at 0.4, 1.5, and 2.7 μs. The mass fraction contours are 0.8 and 0.5.
13. The calculated three-dimensional pressure and mass fraction contours for three initiators in PBX 9502. The pressure contours are shown for 200, 150, and 100 kbar at 1.5, 3.1, and 4.5 μs. The mass fraction contours are 0.8 and 0.5.
14. The isobar and mass fraction cross sections for layer j of 9 are shown for two initiators at 1.34 μs. The isobar interval is 50 kbar. The mass fraction interval is 0.1.
15. The isobar and mass fraction cross sections for layer j of 9 are shown for two initiators at 1.78 μs. The isobar interval is 50 kbar. The mass fraction interval is 0.1.
16. The isobar and mass fraction cross sections for layer j of 9 are shown for two initiators at 2.66 μs. The isobar interval is 50 kbar. The mass fraction interval is 0.1.
17. The isobar and mass fraction cross sections for layer j of 11 are shown for three initiators at 1.78 μs. The isobar interval is 50 kbar. The mass fraction interval is 0.1.
18. The isobar and mass fraction cross sections for layer j of 11 are shown for three initiators at 3.10 μs. The isobar interval is 50 kbar. The mass fraction interval is 0.1.

Figure captions (cont)

19. The isobar and mass fraction cross sections for layer j of 11 are shown for three initiators at 4.42 μs. The isobar interval is 50 kbar. The mass fraction interval is 0.1.

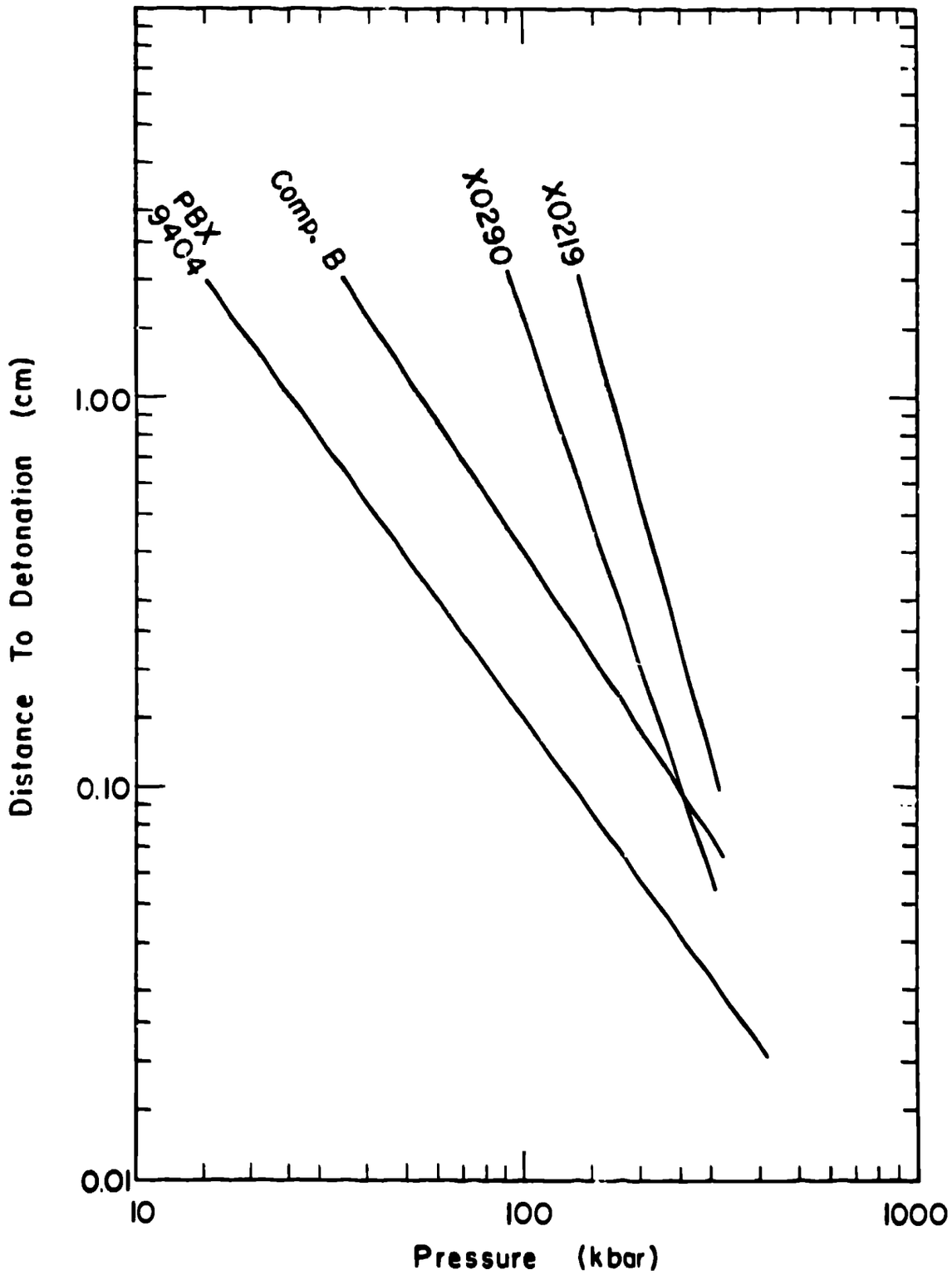
PBX 9404
Comp. B
X0290
X0219
1.00
0.10
0.01
10
100
1000
Distance To Detonation (cm)
Pressure (kbar)

Fig. 1 - Tarver

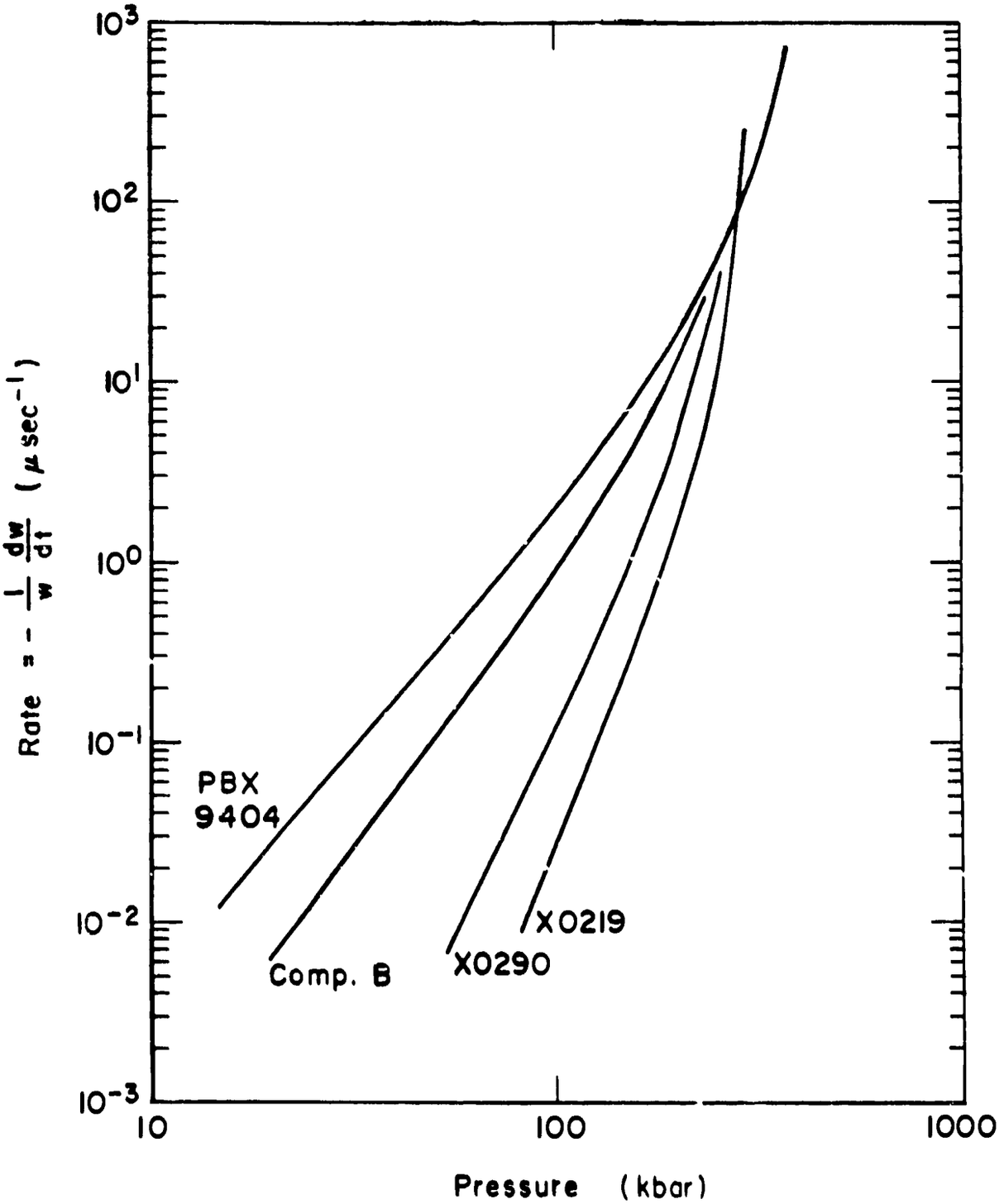
10^3
10^2
10^1
10^0
10^{-1}
10^{-2}
10^{-3}
Rate = $-\frac{1}{w}\frac{dw}{dt}$ (μsec^{-1})
PBX 9404
Comp. B
X0290
X0219
10
100
1000
Pressure (kbar)

Fig. 2 - Trulio

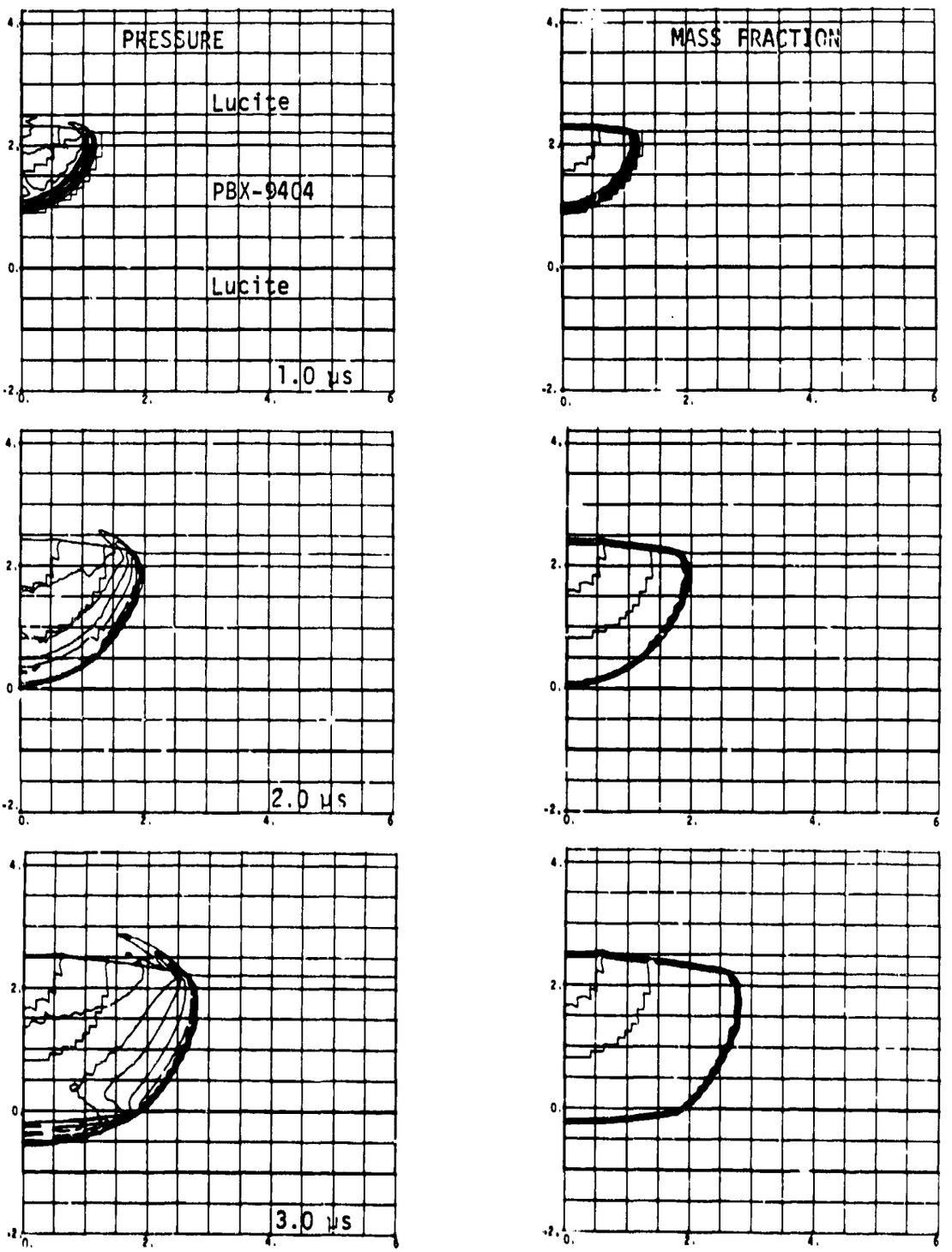
PRESSURE
Lucite
PBX-9404
Lucite
1.0 μs
MASS FRACTION
2.0 μs
3.0 μs

Fig. 3 - Trader

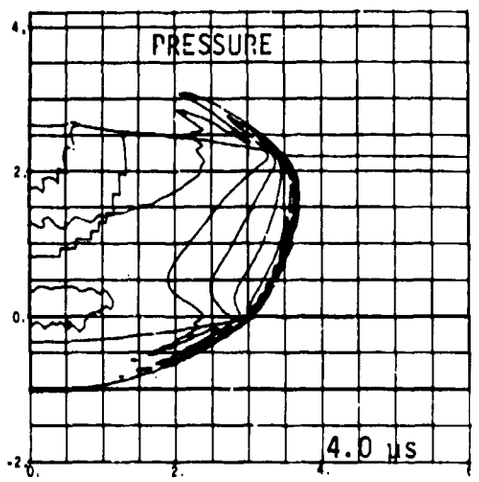
PRESSURE
4.0 μs

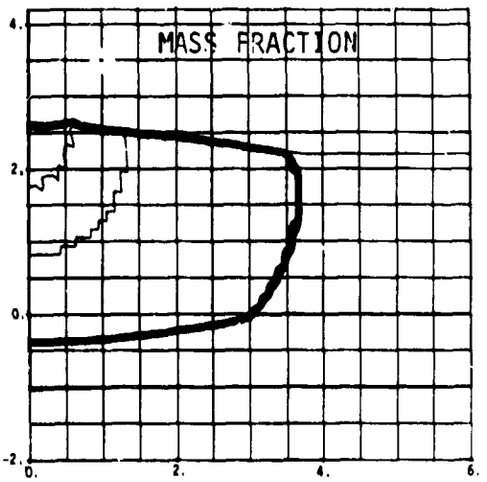
MASS FRACTION

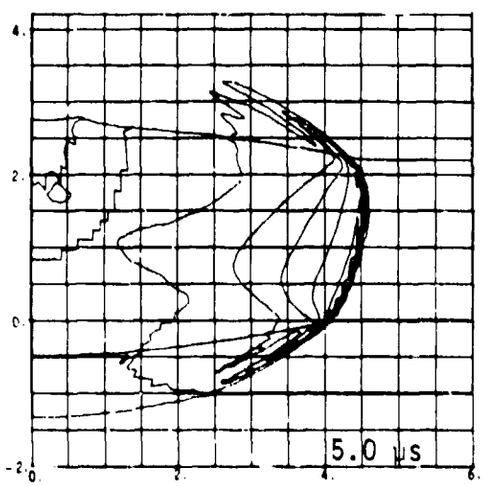
5.0 μs

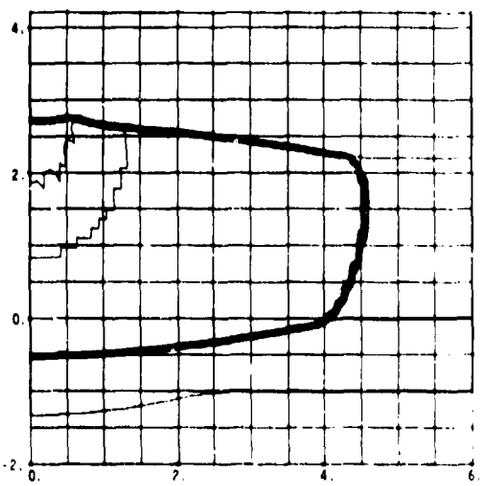

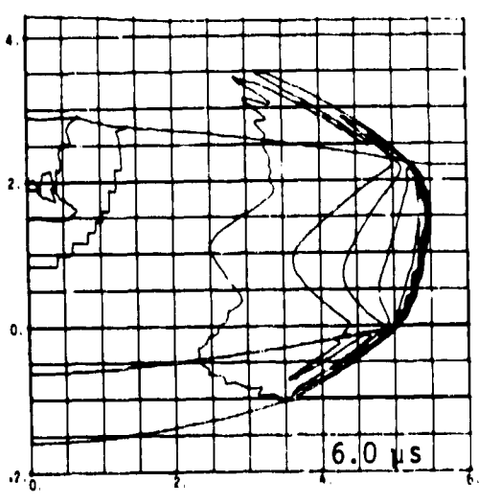
6.0 μs

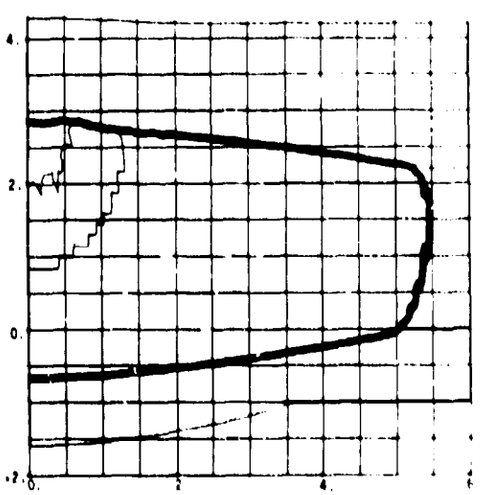

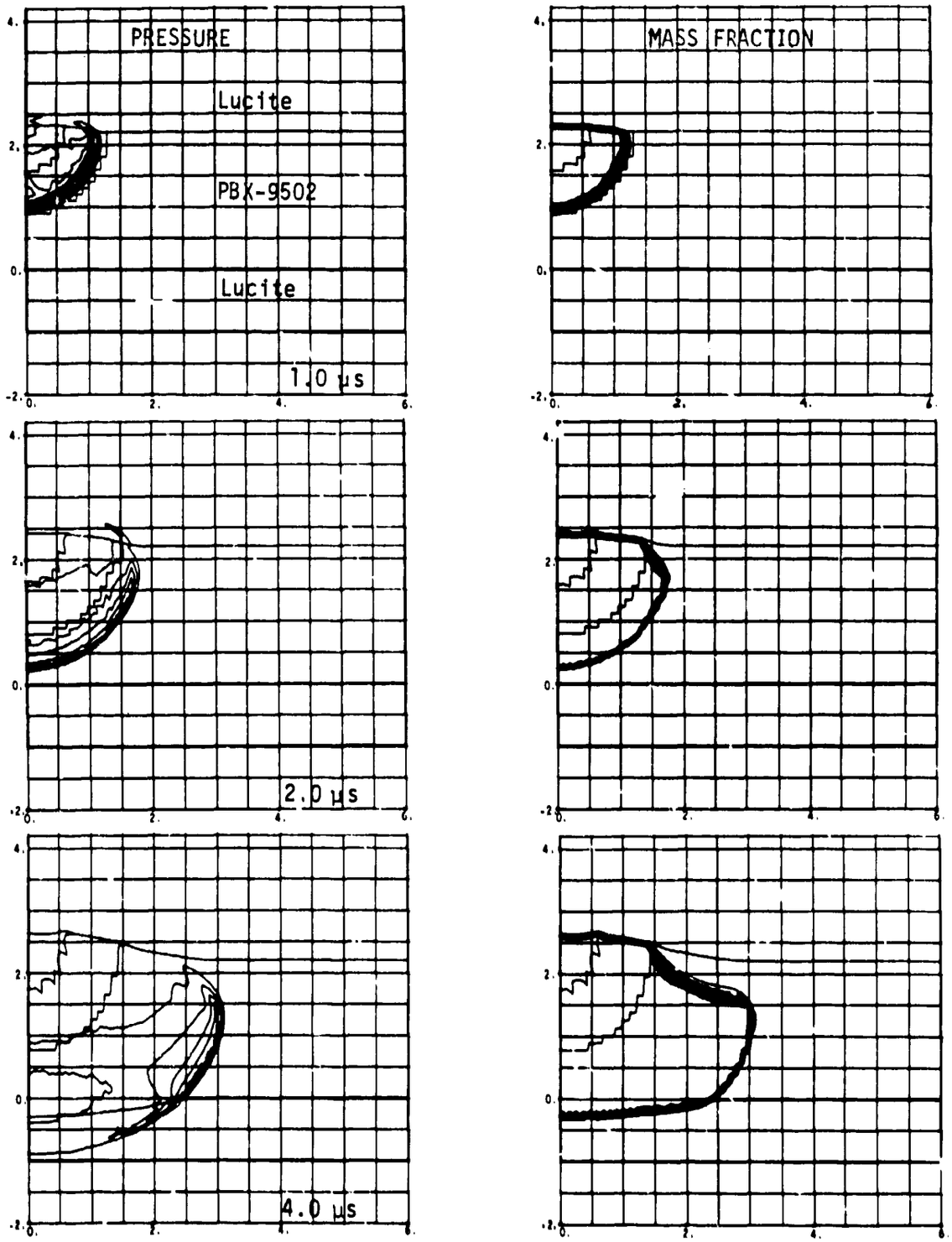
PRESSURE
MASS FRACTION
Lucite
PBX-9502
Lucite
1.0 μs
2.0 μs
4.0 μs

Lig. 4. Mader

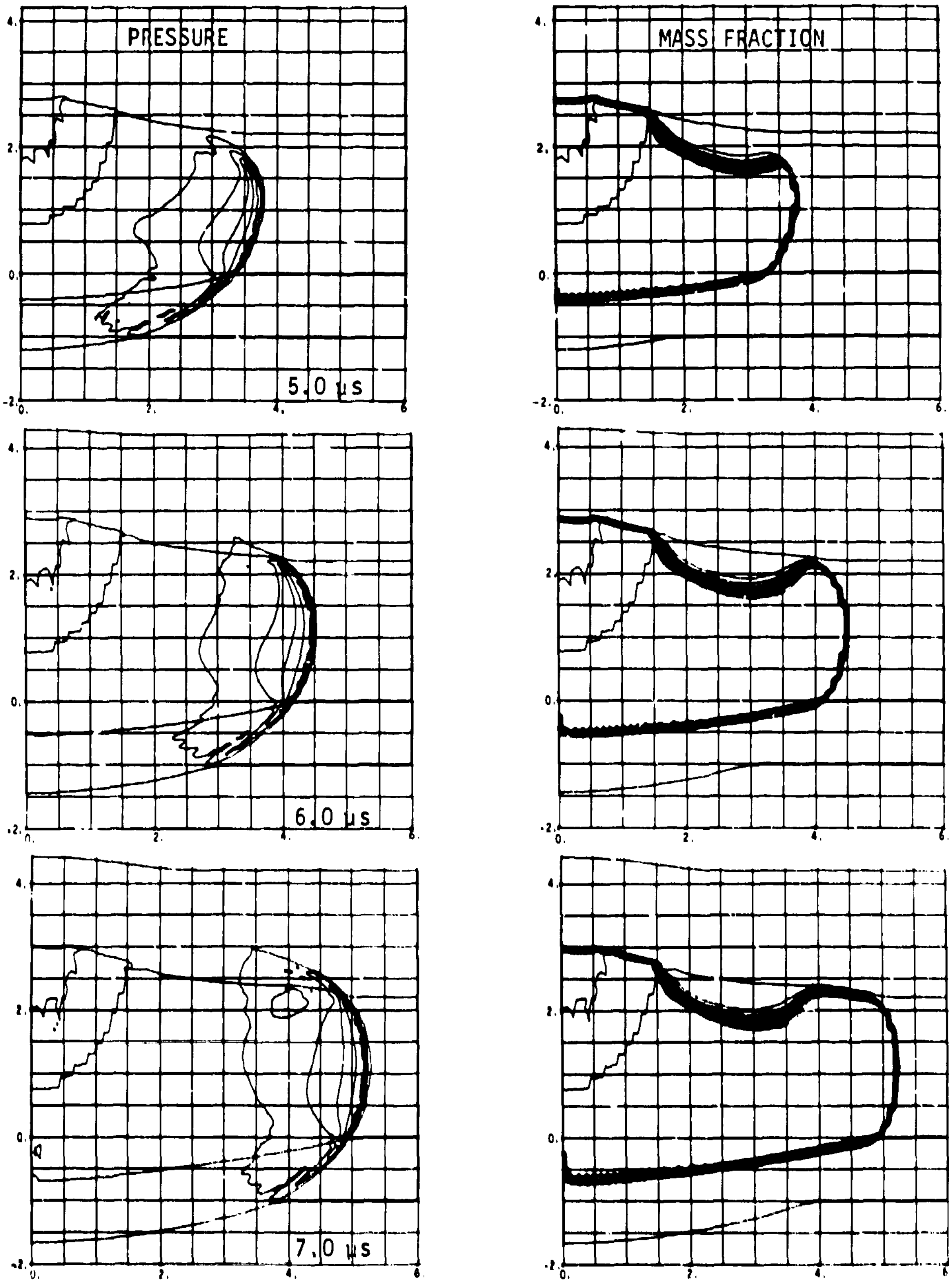

PRESSURE
MASS FRACTION
5.0 μs
6.0 μs
7.0 μs
4.
2.
0.
-2.
0.
2.
4.
6.

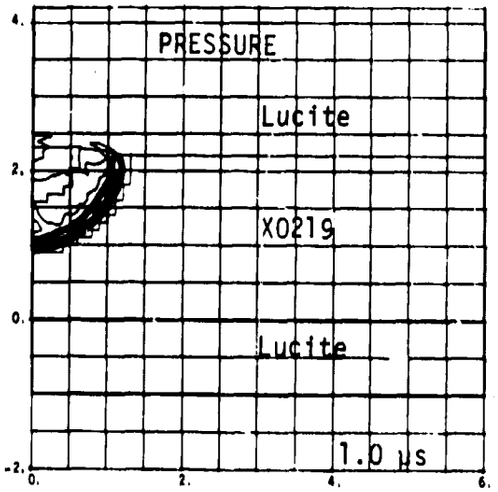
PRESSURE
Lucite
X0219
Lucite
1.0 μs

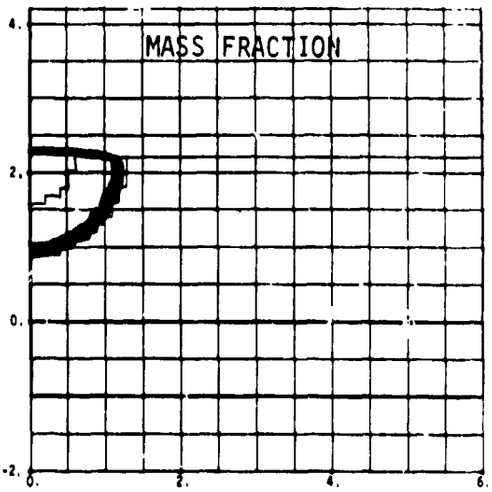
MASS FRACTION

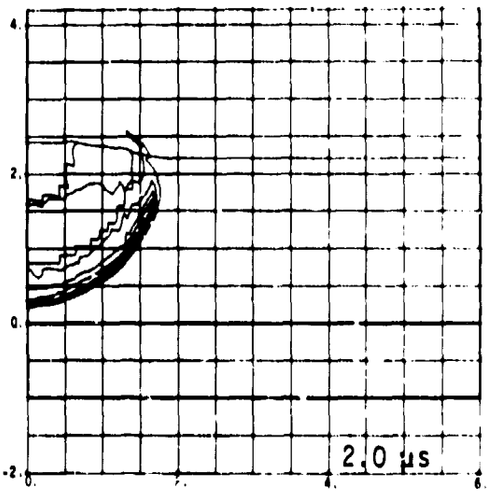
2.0 μs

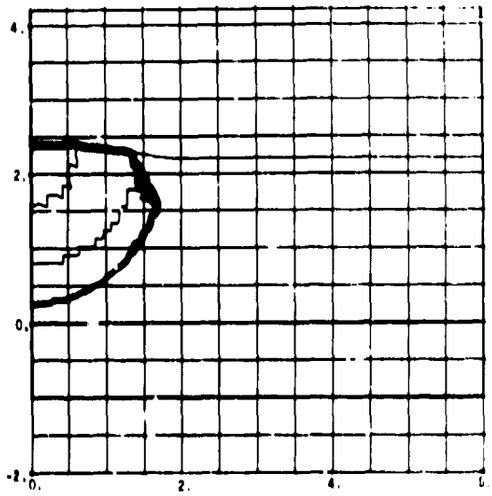

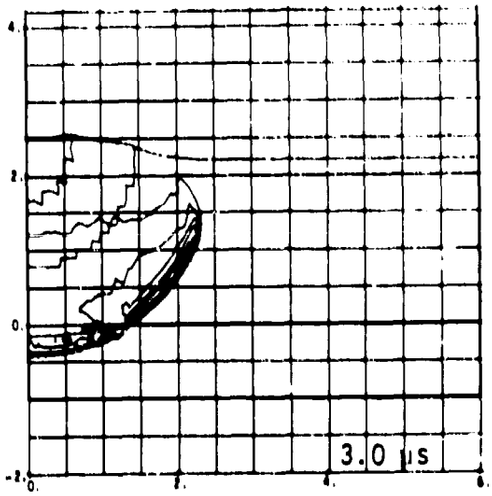
3.0 μs

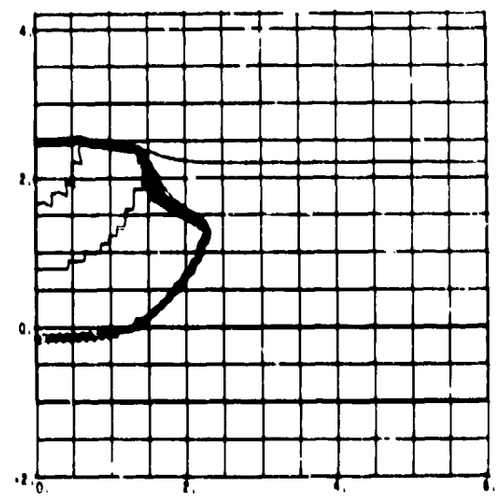

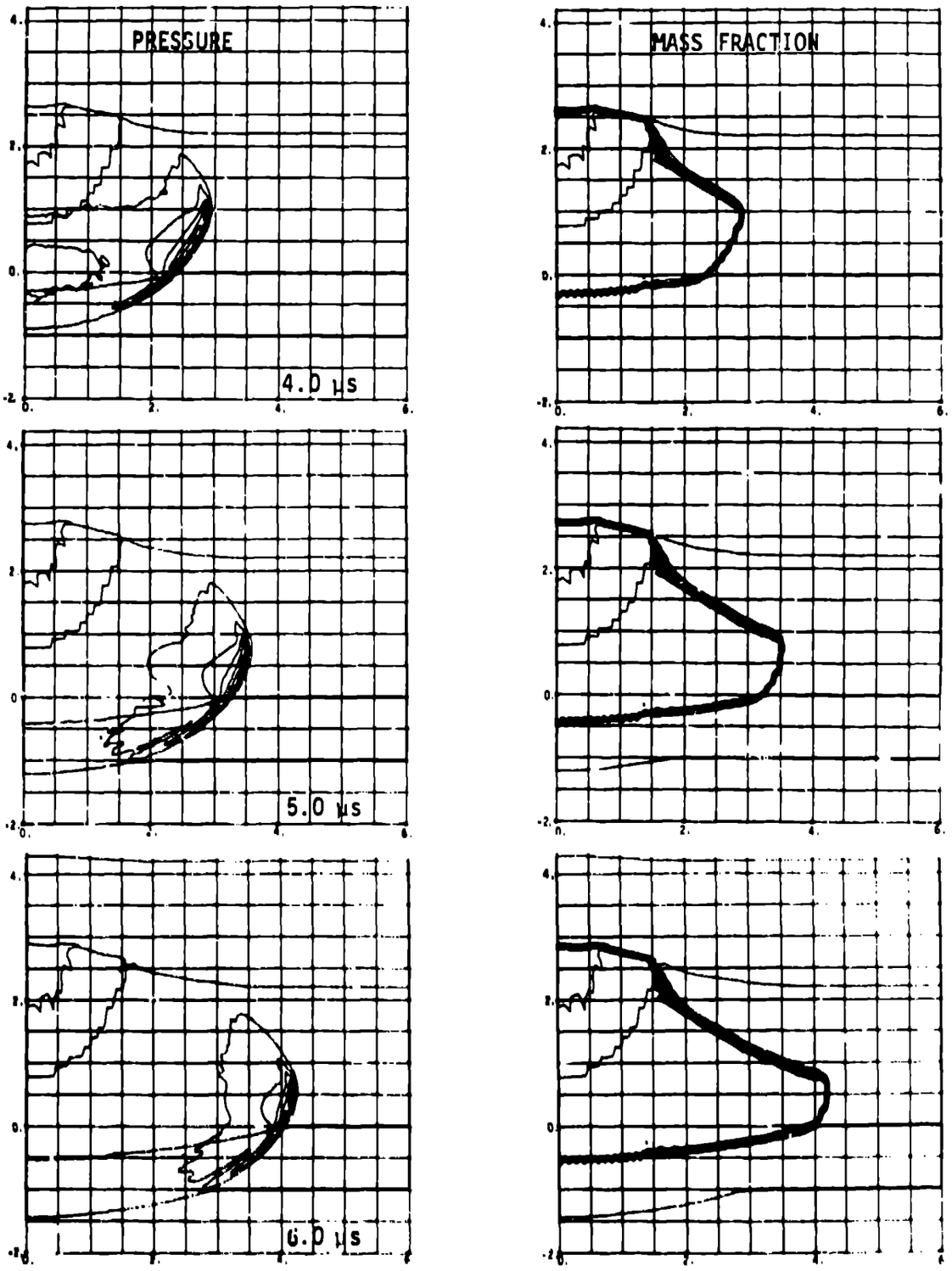

Fig 5 (cont) - Bruder

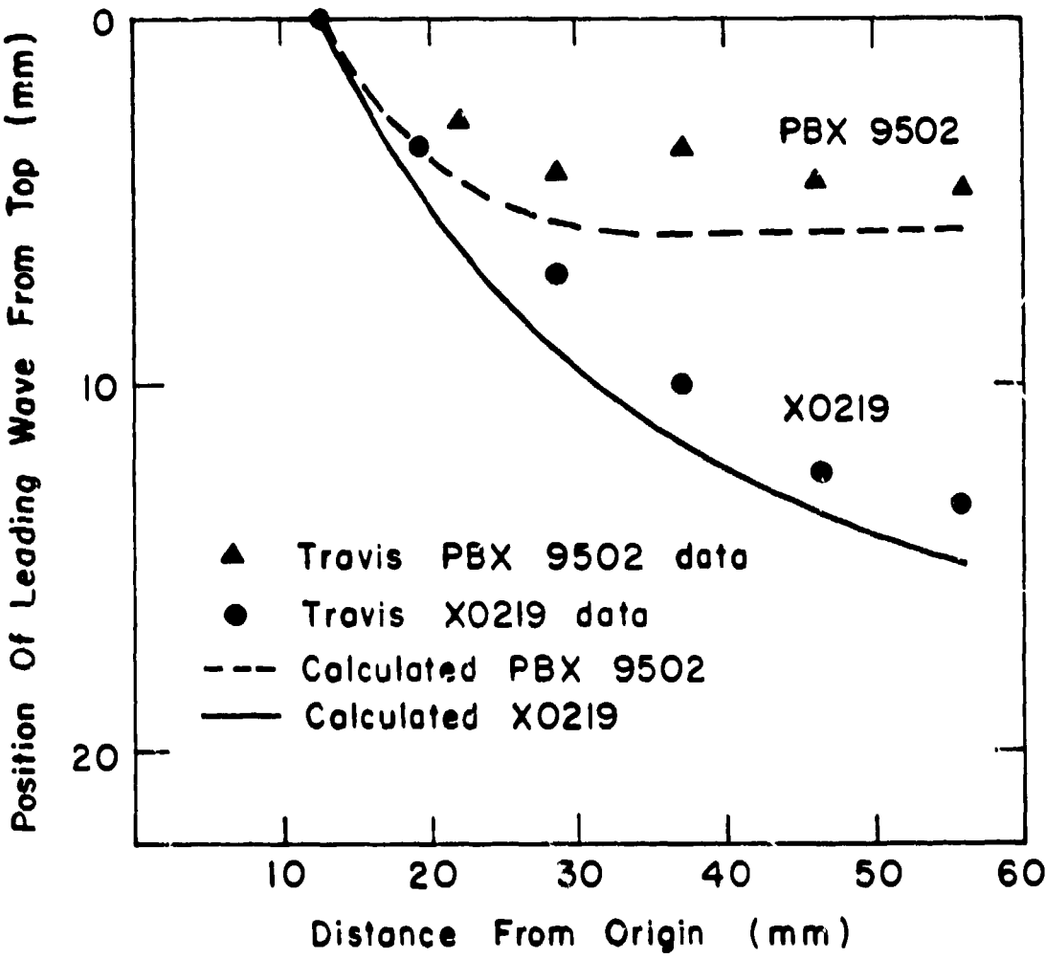
Position Of Leading Wave From Top (mm)
0
10
20
10
20
30
40
50
60
Distance From Origin (mm)
PBX 9502
X0219
Travis PBX 9502 data
Travis X0219 data
Calculated PBX 9502
Calculated X0219

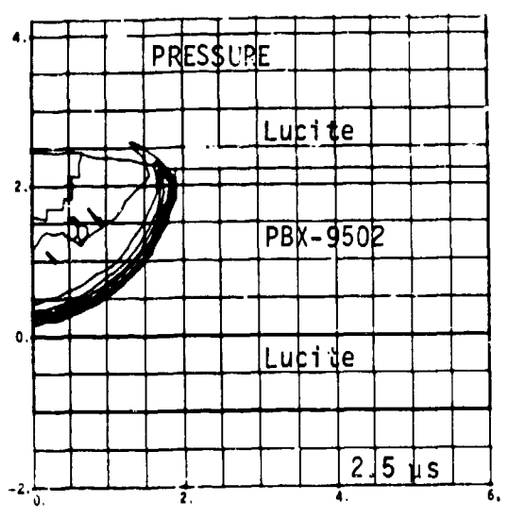
PRESSURE
Lucite
PBX-9502
Lucite
2.5 μs

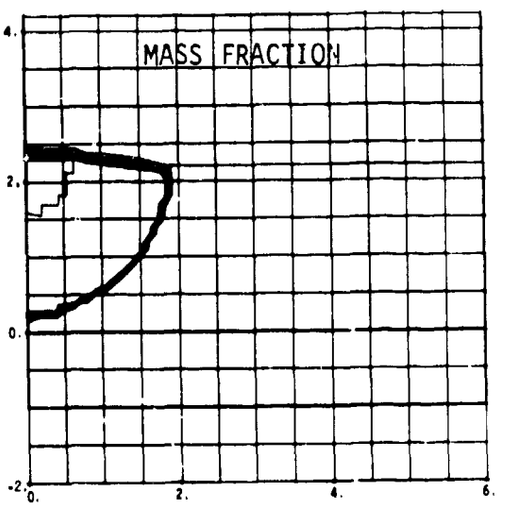
MASS FRACTION

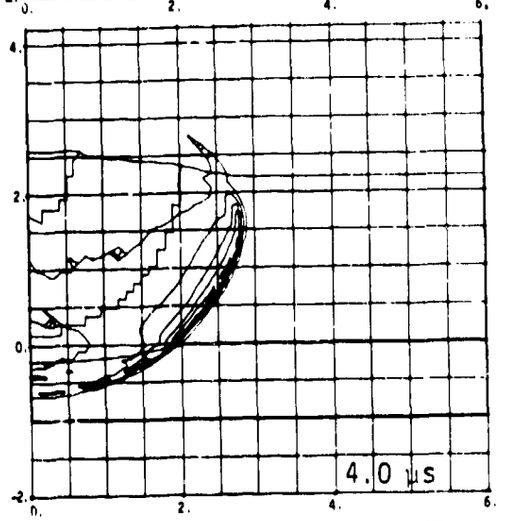
4.0 μs

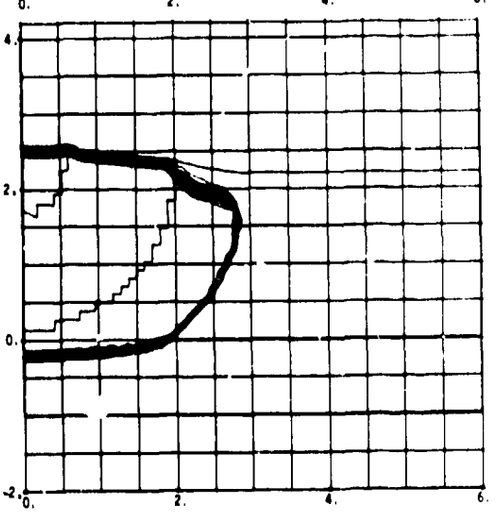

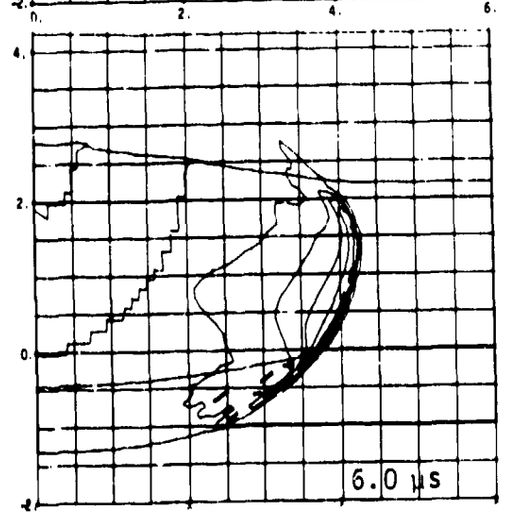
6.0 μs

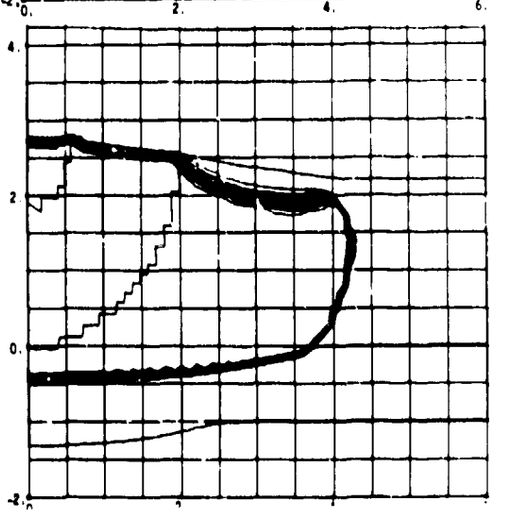

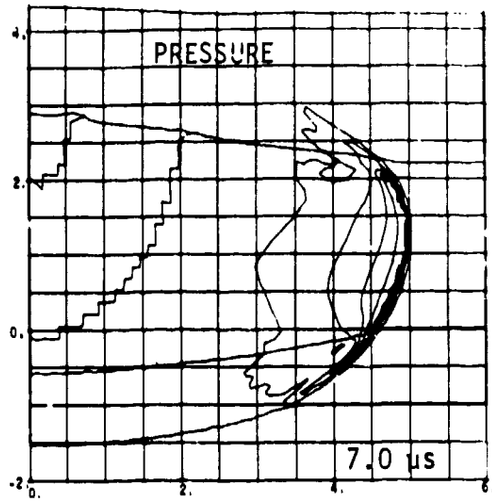
PRESSURE
7.0 μs

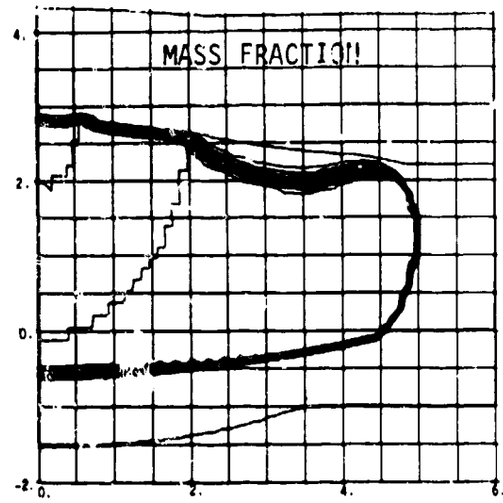
MASS FRACTION

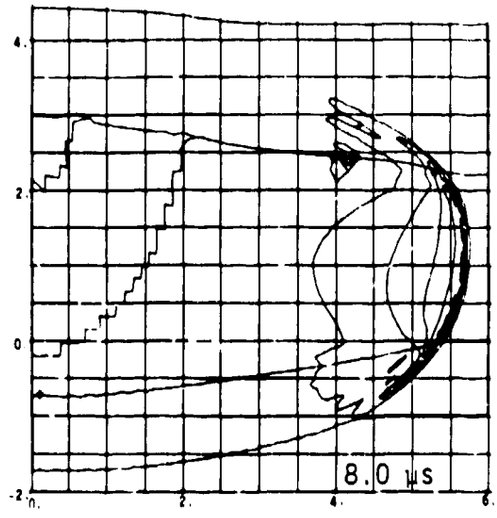
8.0 μs

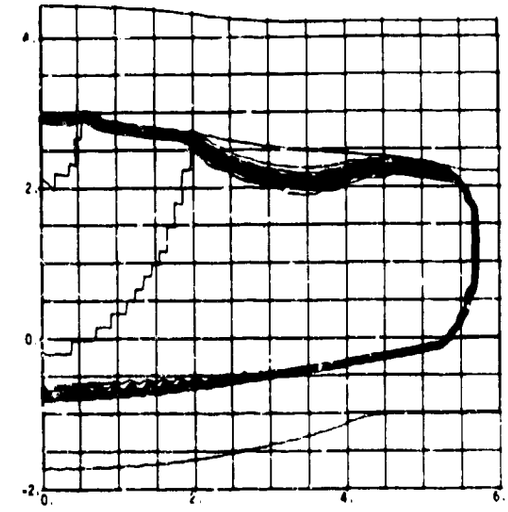

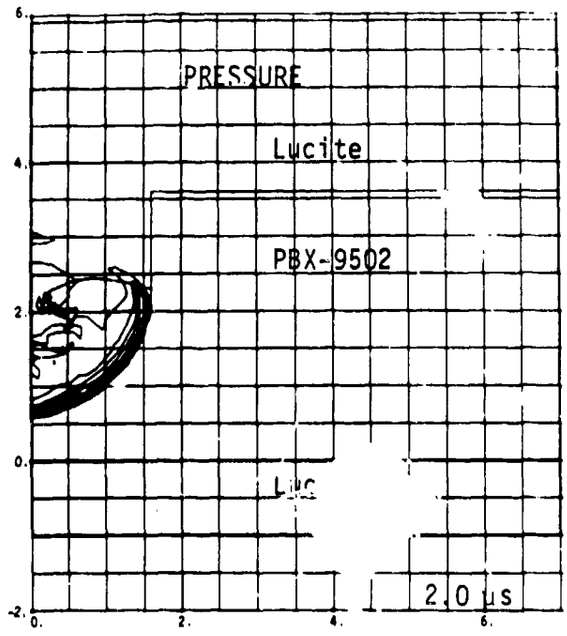
PRESSURE
Lucite
PBX-9502
2.0 μs

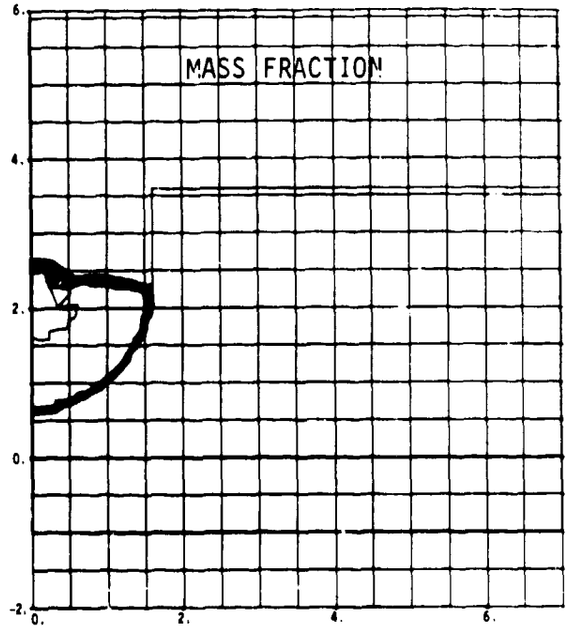
MASS FRACTION

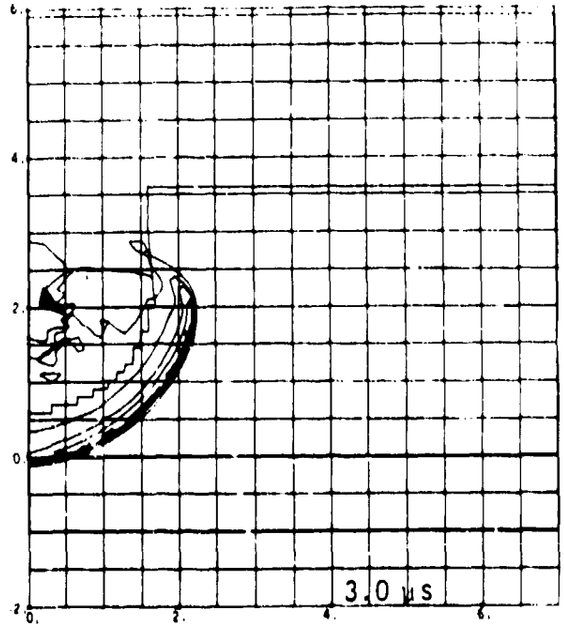
3.0 μs

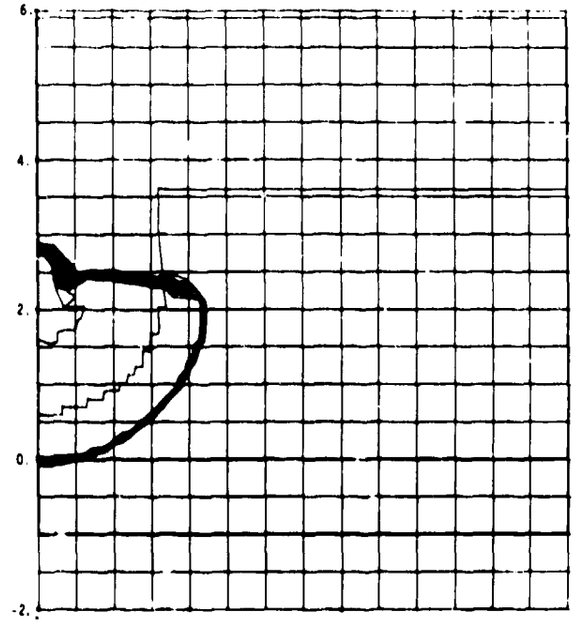

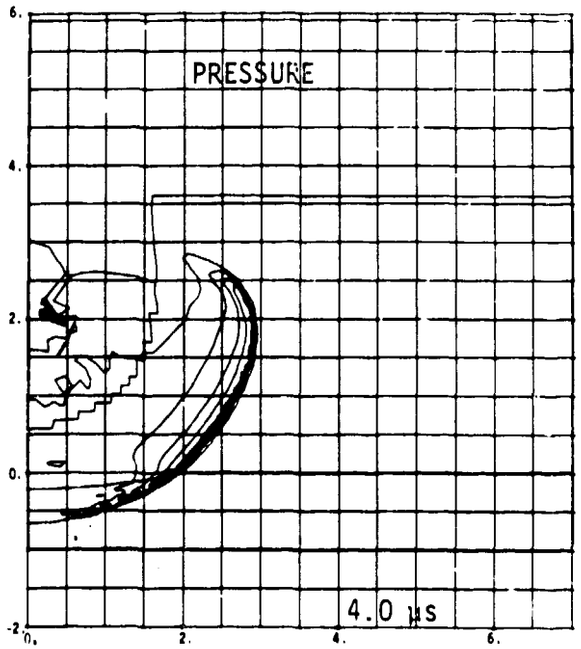

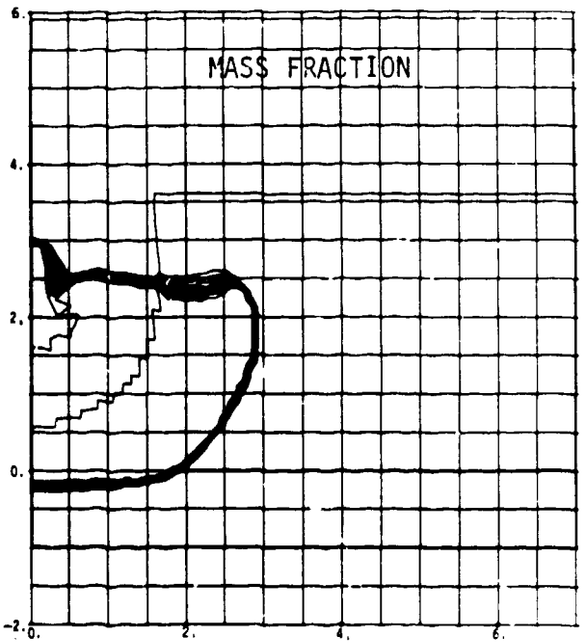

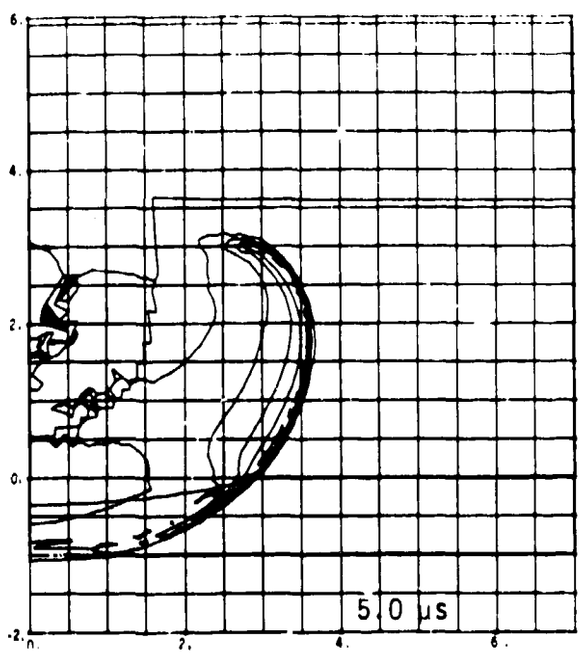

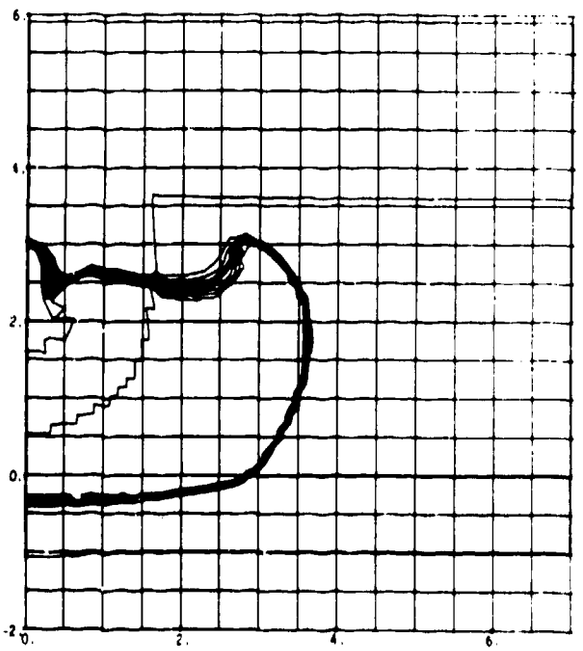

Fig. 8 (cont) - Trudeau

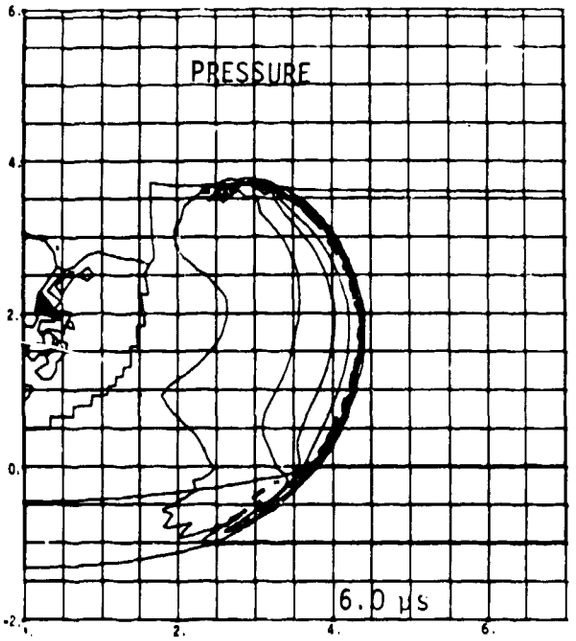
PRESSURE
6.0 μs

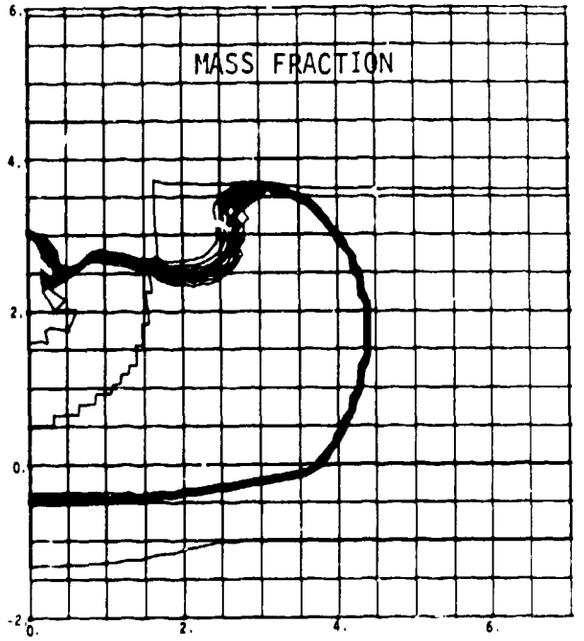
MASS FRACTION

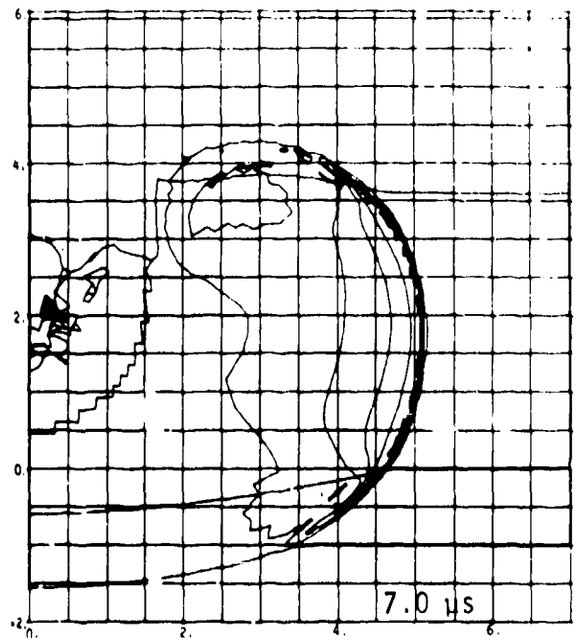
7.0 μs

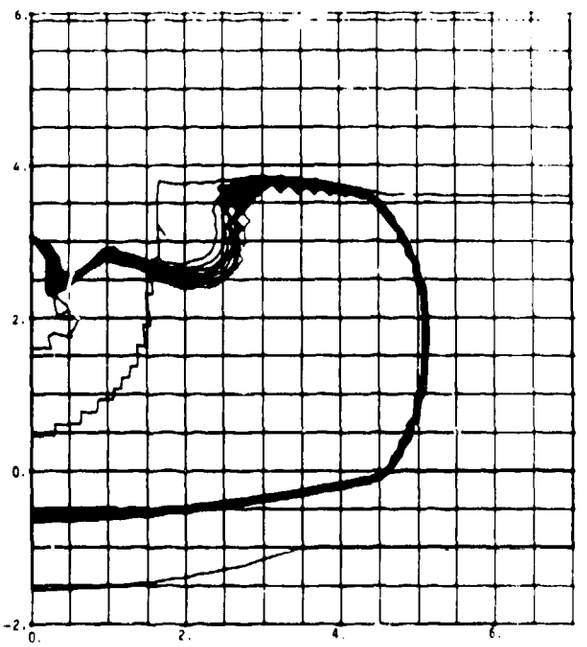

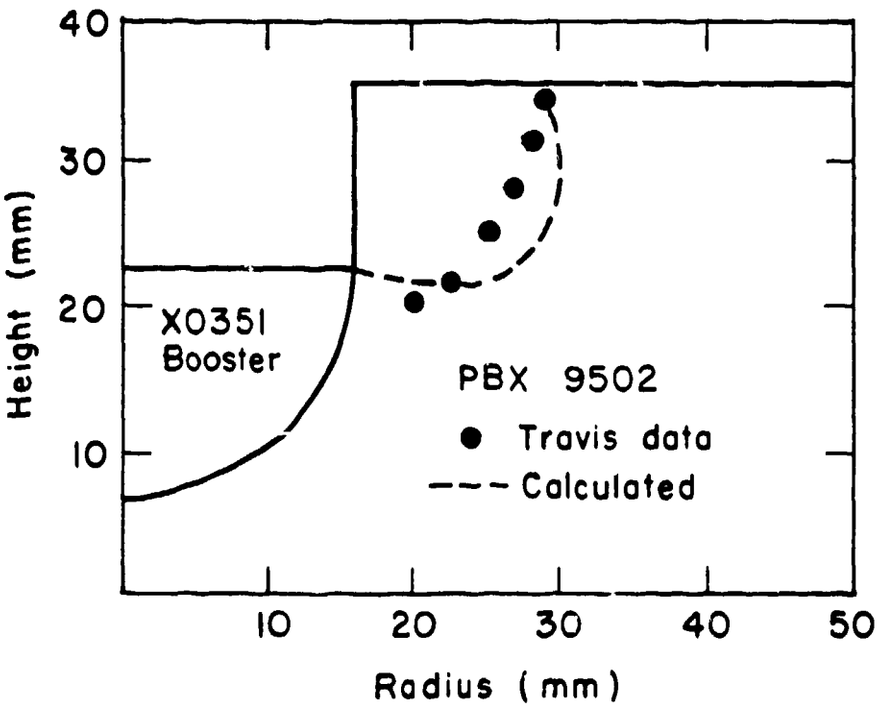
40
30
20
10
Height (mm)
X0351
Booster
PBX 9502
Travis data
Calculated
10
20
30
40
50
Radius (mm)

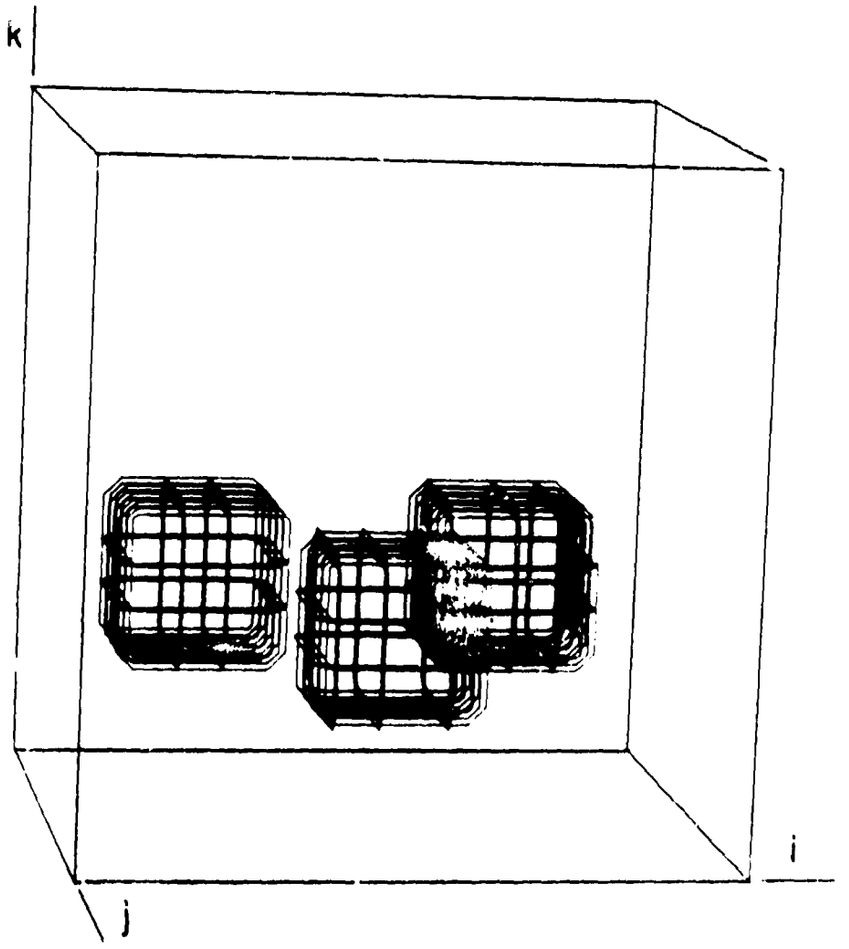
k
i
j

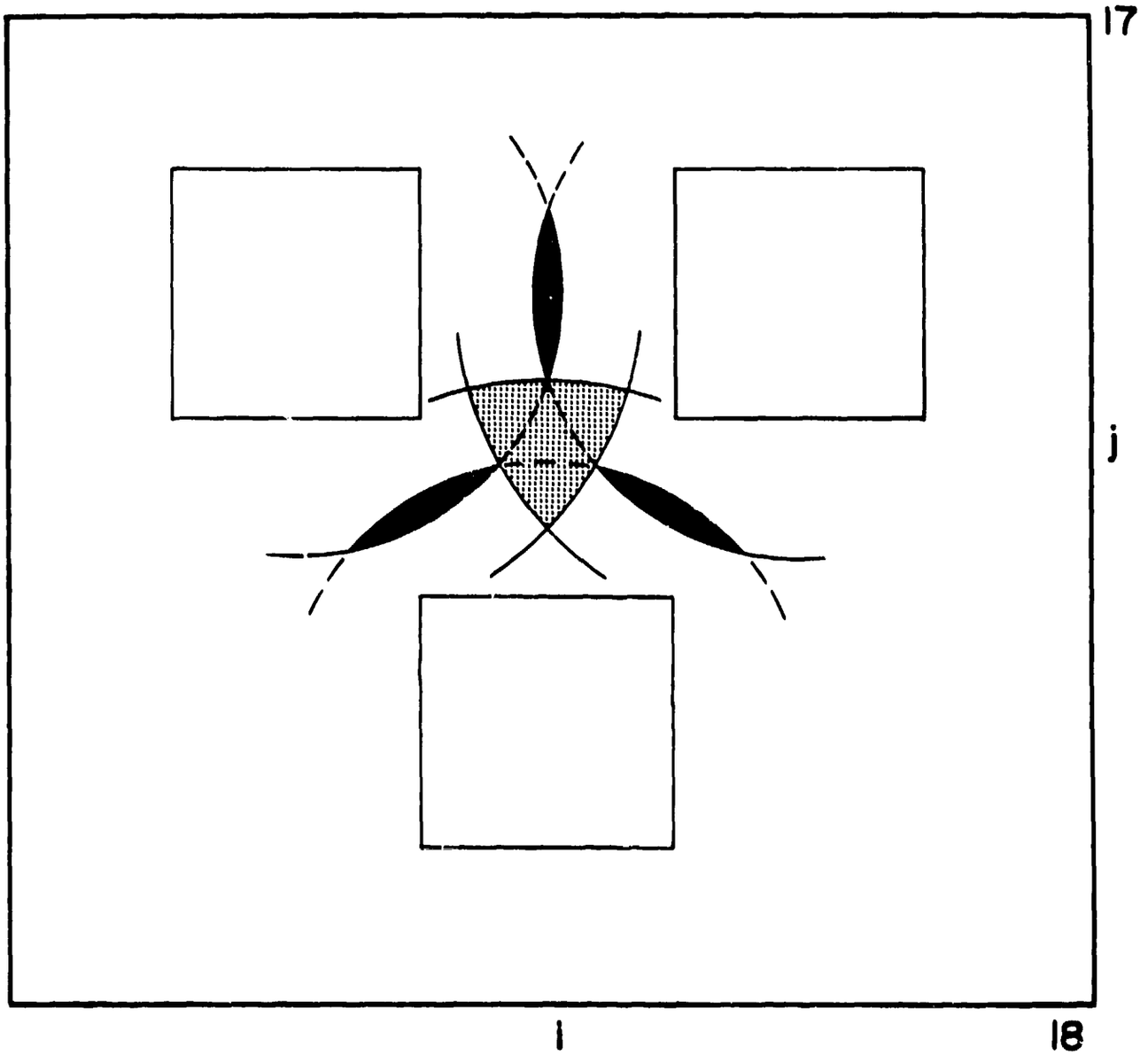
17
j
1
18

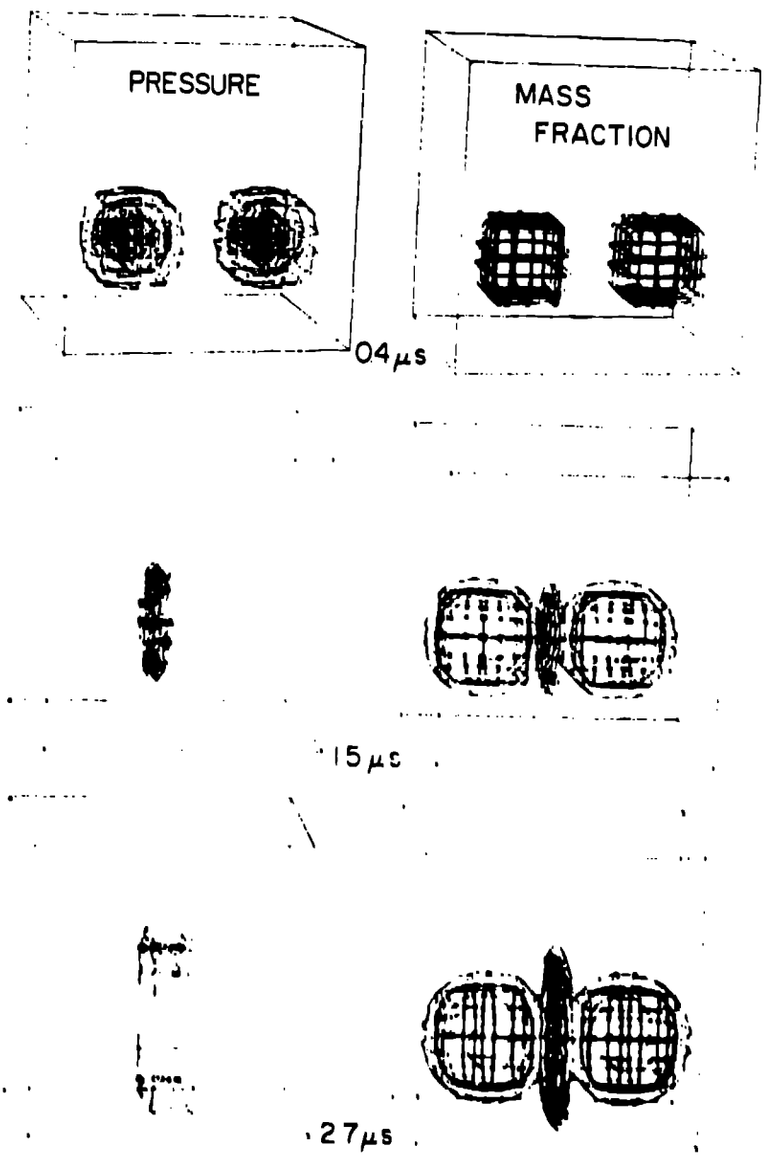
PRESSURE
MASS
FRACTION
.04 μs
.15 μs
.27 μs

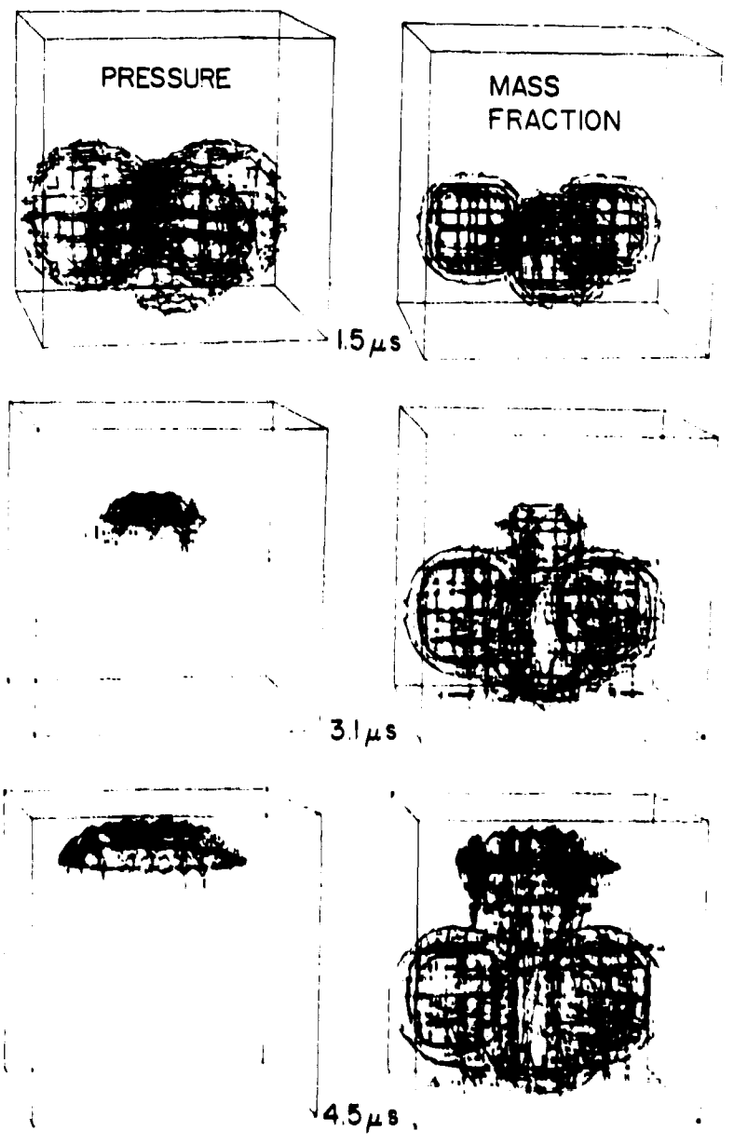

Fig. 13 - Sanders

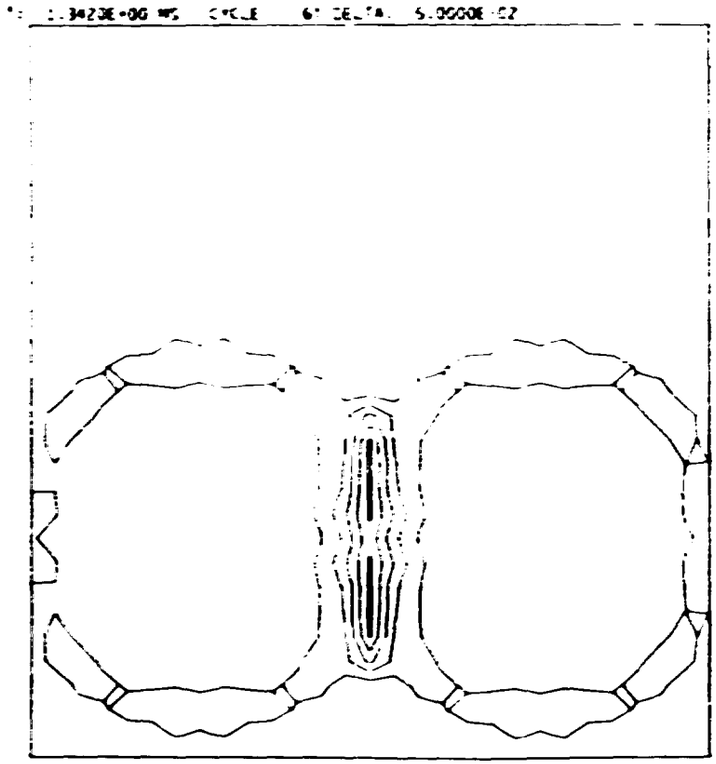

PRESSURE (MEGABARS) J= 9

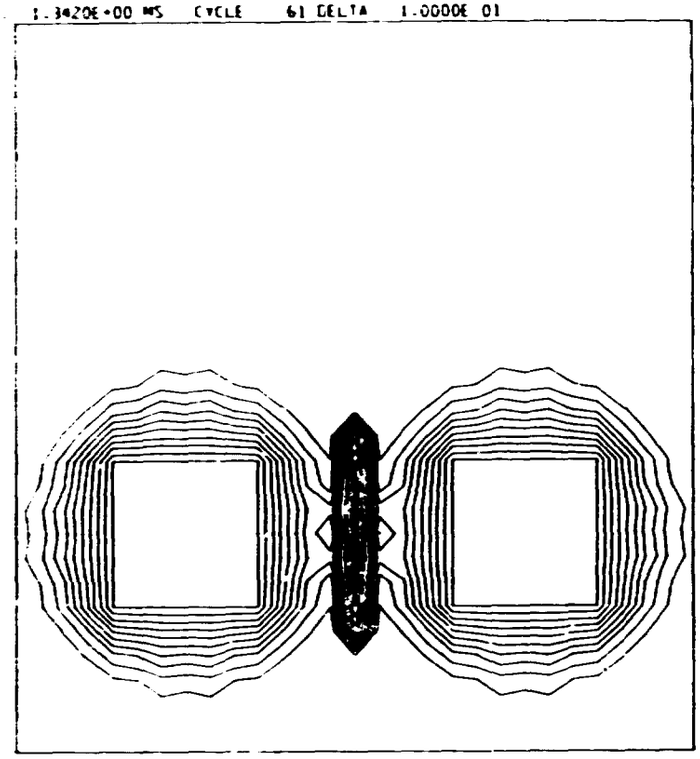

BURN MASS FRACTION J= 9

Fig. 14 - Trader

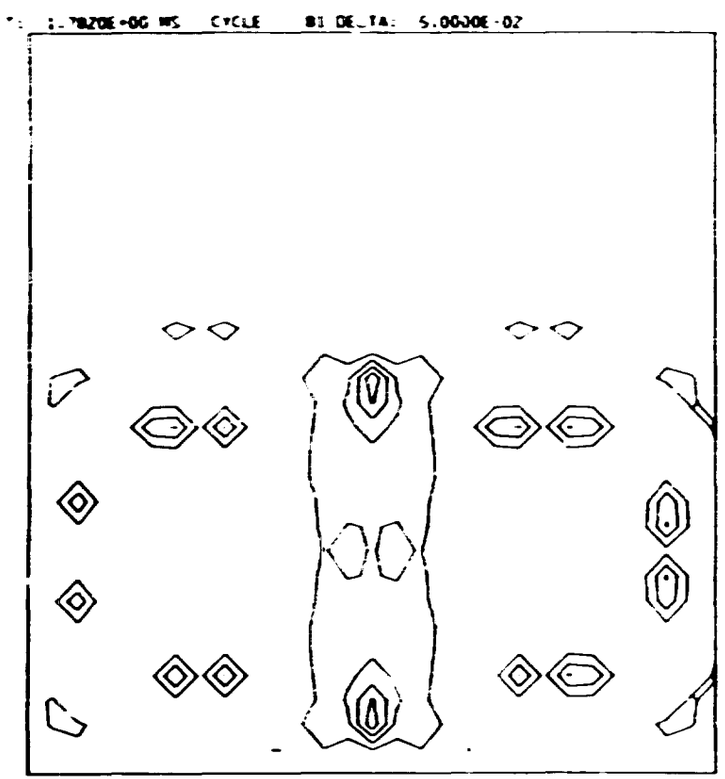

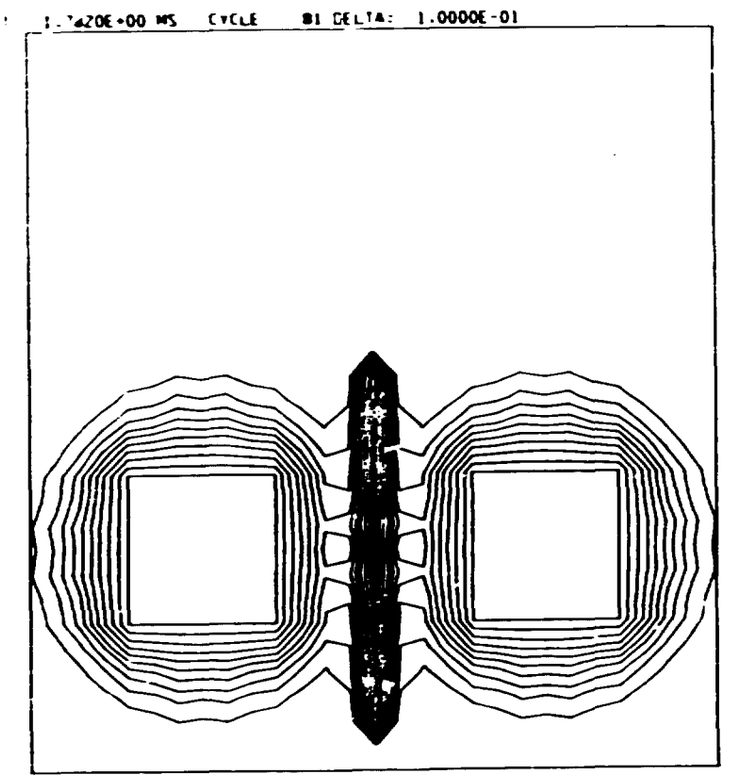

Fig. 15 - Trader

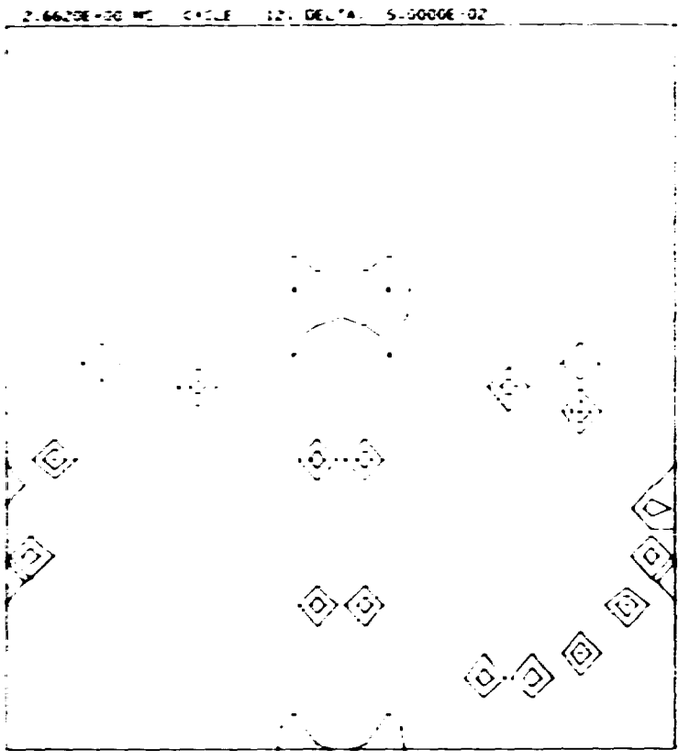

PRESSURE (MEGABARS) J= 9

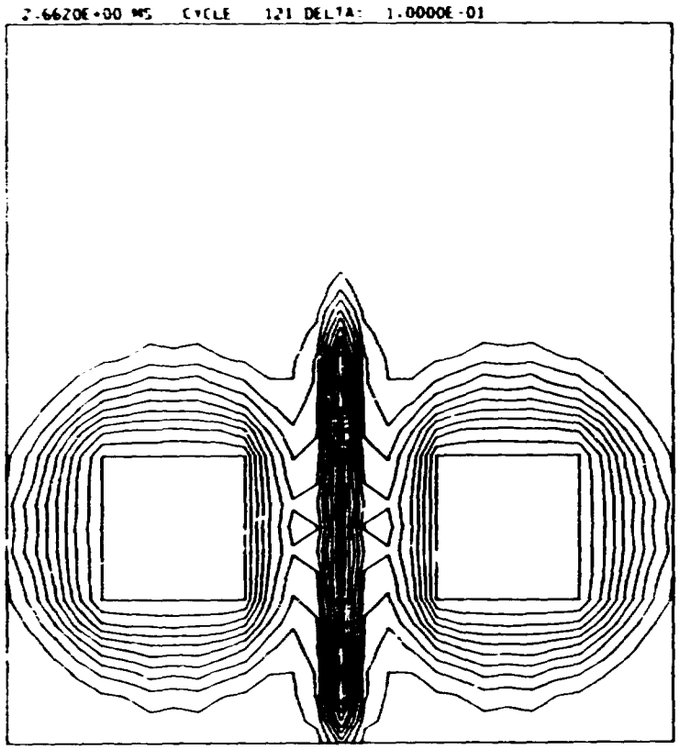

BURN MASS FRACTION J= 9

Fig. 16 - Mader

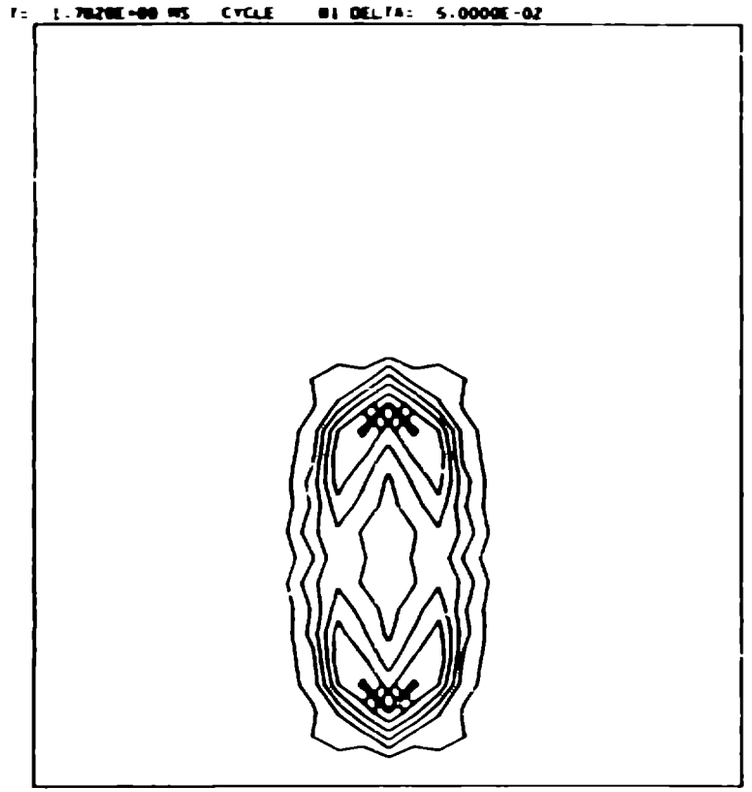

PRESSURE (MEGABARS) J= 11

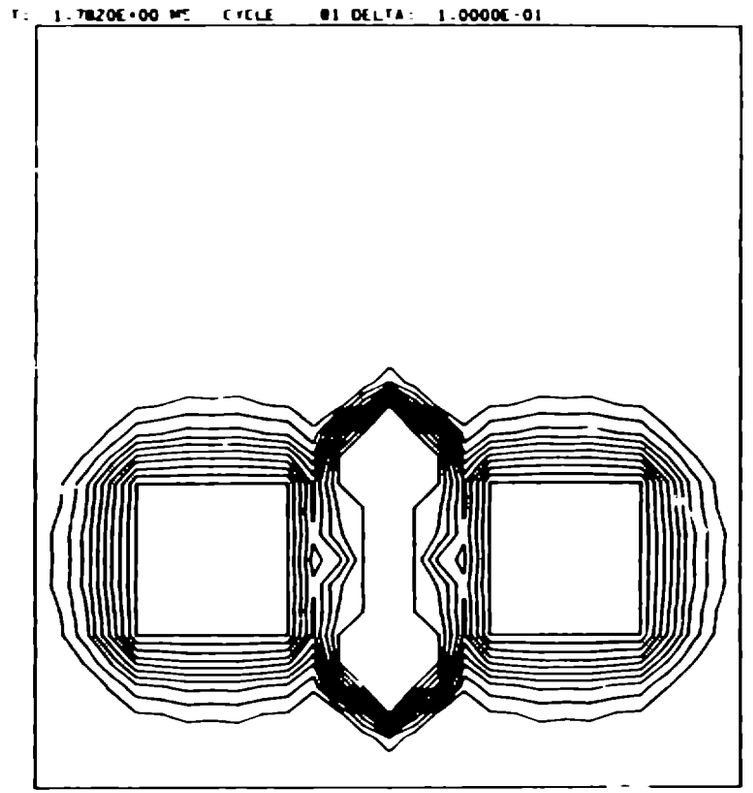

BURN MASS FRACTION J= 11

Fig. 17 - Two-D.

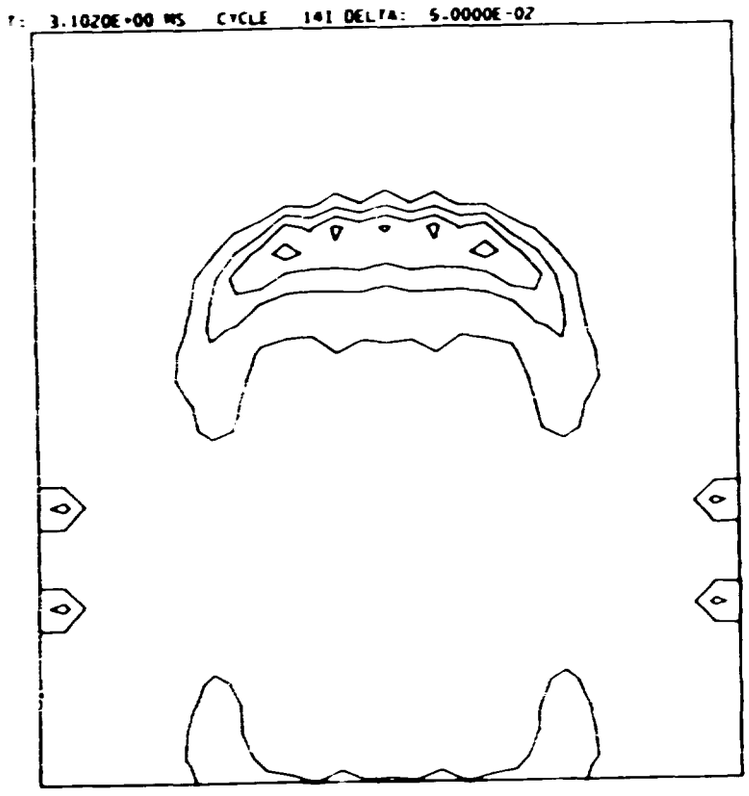
T: 3.1020E+00 MS CYCLE 141 DELTA: 5.0000E-02
PRESSURE (MEGABARS)
J= 11

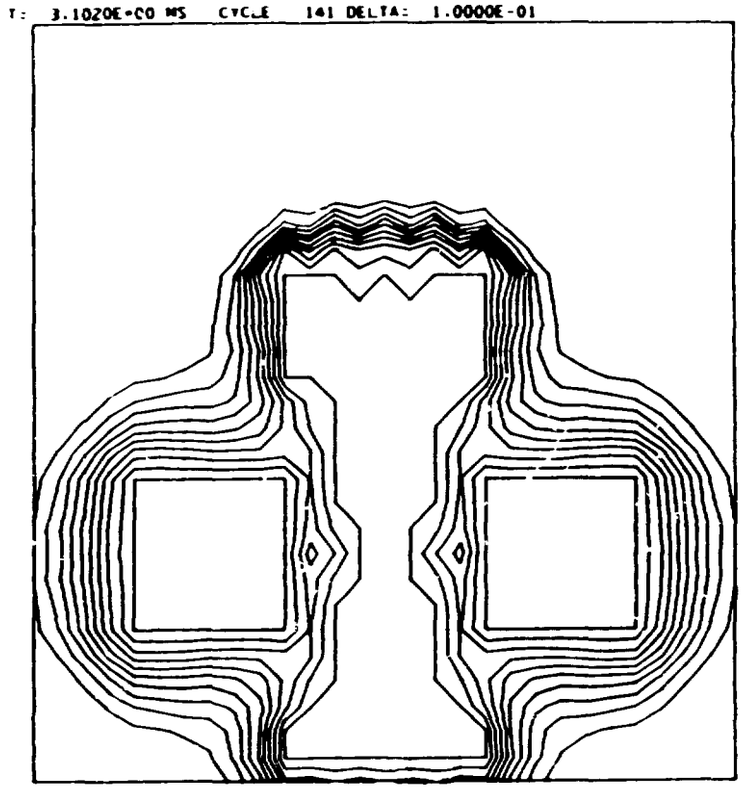
T: 3.1020E+00 MS CYCLE 141 DELTA: 1.0000E-01
BURN MASS FRACTION
J= 11

Fig. 18 - Mader

#

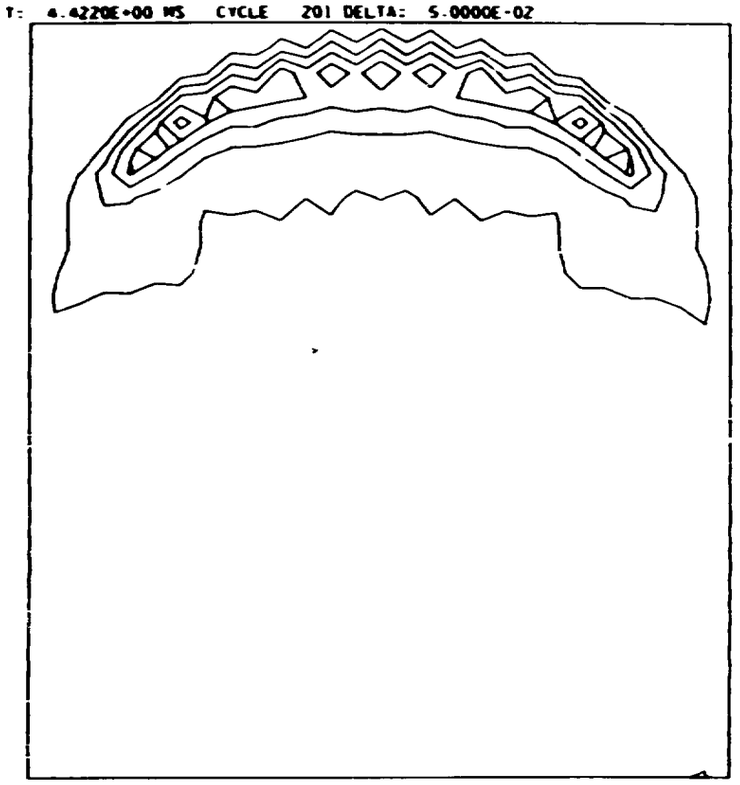
T= 4.4220E+00 MS CYCLE 201 DELTA= 5.0000E-02
PRESSURE (MEGABARS)
J= 11

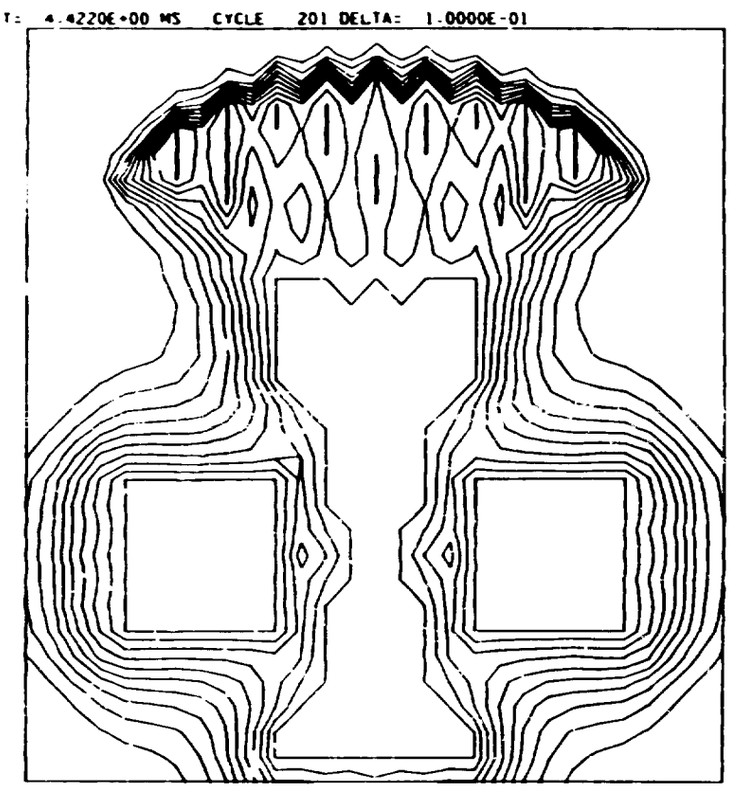
T= 4.4220E+00 MS CYCLE 201 DELTA= 1.0000E-01
BURN MASS FRACTION
J= 11

Fig. 19. 2-D...